Read Versus Flat Doping Profile Structures for the Realization of Reliable High-Power, High-Efficiency 94 GHz IMPATT Sources

CHRISTOPHE DALLE AND PAUL-ALAIN ROLLAND

Abstract —The potential RF performance of various types of silicon IMPATT homojunction structures has been systematically investigated in order to define the one that is most efficient for reliable high-power, high-efficiency CW generation in the 94 GHz window. The comparison has been carried out by means of an IMPATT oscillator model accounting, in a self-consistent manner, for both the thermal limitation and the diode impedance matching. The main result is that in contrast to lower operating frequencies, the realization of a Read doping profile does not improve the RF performance level compared to flat doping profile structures. High RF emitted performance has been predicted under optimum operating conditions. In addition, the fundamental influences on RF performance of both the diode thermal resistance and RF losses have been quantified.

I. Introduction

THE RECENT development of microwave systems in the millimeter-wave range has revived interest in avalanche and transit time diodes (IMPATT) [1]. In fact, in the present state of semiconductor device technology, these diodes remain the most powerful structures for the realization of millimeter-wave solid-state high-power sources. In the 94 GHz window, theoretical studies as well as experimental results have demonstrated that silicon yields the highest performance levels [2], [3]. Moreover flat doping profile structures are presently the most commonly grown structures for commercially available devices. The state of the art with double-drift flat doping structures at 94 GHz is an output power level up to 980 mW (however, near burnout) and more recently 700 mW associated with 11% efficiency at safe junction operating temperatures [4]–[6]. However, on the basis of classical IMPATT design concepts, the flat doping profile structure is not the most powerful [7]. The electric field distribution in the active zone of such diodes is not optimum since the avalanche region width, in which the RF power generation is low, is a significant fraction of the entire active zone thickness. By contrast, Read doping profile structures yield a better electric field spatial distribution since the avalanche zone can be better confined. However, the realization of such structures requires rigorous control of the epitaxial growth due to the implementation of highly doped narrow spikes. This difficulty is increased by the submicron dimensions of the active zone at millimeter-wave operating frequencies.

Recent reports have demonstrated that high-power 94 GHz Read doping profile silicon IMPATT diodes can be realized by means of molecular beam epitaxy, and RF power levels up to 910 mW have been achieved [8], [9]. Since all the experimental power levels reported are close together, it is of interest to develop an accurate comparative evaluation of the potential performance of the various Read and flat doping profile silicon IMPATT structures at 94 GHz. This is the main purpose of this paper. Each structure considered has been optimized by means of an IMPATT oscillator model accounting, in a self-consistent manner, for both the thermal limitation and the diode impedance matching conditions. The potential RF performances are then presented, compared, and discussed. Finally, since the oscillator net output power depends on both thermal limitations and diode-to-load energy transfer efficiency, the influence of the thermal resistance and RF losses on RF performance has been quantified.

II. The IMPATT Oscillator Model

From an electrical point of view, the IMPATT oscillator has been simply considered as an IMPATT diode connected to a load impedance. This configuration makes it possible to study the RF performance at a given frequency for various bias and load conditions and to consider that the diode is driven with a sinusoidal voltage [10]. Following this electrical configuration the IMPATT oscillator model basically relies on a p-n junction device model which has been incorporated in a numerical sequence leading to self-consistent operating conditions and accounting for thermal limitations, bias effect, and impedance matching [6].

The IMPATT diode model used in this study is a numerical unidimensional macroscopic drift-diffusion model. The main feature of this model is that the carrier

Manuscript received December 20, 1988; revised November 29, 1989. This work was supported by the Direction de la Recherche et Etudes Techniques under Contract D.R.E.T. 83–110.

The authors are with the Centre Hyperfréquences et Semiconducteurs, Université des Sciences et Techniques de Lille Flandres Artois, Bât. P4-59655 Villeneuve d'Ascq Cedex, France.

IEEE Log Number 8933769.

0018-9480/90/0400-0366$01.00

TABLE 1
TECHNOLOGICAL PARAMETERS OF THE 94 GHz SINGLE- AND DOUBLE-DRIFT FLAT DOPING PROFILE STRUCTURES

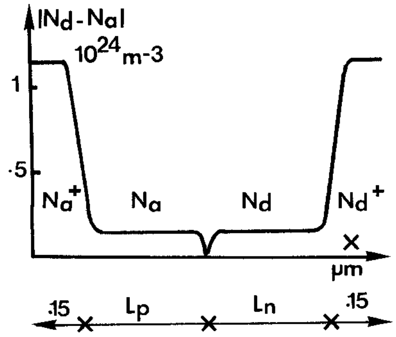

Diode	N_a	N_d	L_n	L_p
	$10^{23} m^{-3}$		μm	
DDR1	2	2	.23	.23
DDR2	1.5	1.5	.24	.3
SDR1		1.5	.35	

kinetics are described on the entire semiconductor structure since the heavily doped regions of the collectors are included in the simulations. This allows the description of devices presenting realistic doping profiles. Moreover, boundary values are accurately obtained from carrier thermal equilibrium; the residual current initializing the avalanche process at each RF cycle is not specified but rather results from RF operation. Note that preliminary to this study, the use of a drift-diffusion model versus a nonstationary energy one for silicon IMPATT diode studies at operating frequencies as high as 94 GHz has been justified [11].

This model yields a realistic description of IMPATT oscillator operation. Indeed, both the diode technological parameters (epitaxial layers characteristics, chip area, and thermal resistance) and the operating conditions specified by the experimenter (dc bias current density or junction temperature and load resistance level) are specified, but the diode RF operating parameters (dc bias voltage, RF voltage, and current magnitude) are computed in a self-consistent manner together with the specified data.

III. The Structures Considered

The main classical IMPATT structures have been considered in this study. Theoretically the double-drift structures are the most powerful since they benefit from both the electron and hole transit times. Three kinds of double-drift structures have been considered. The first is the flat doping profile structure (DDR). The second and third ones are the Read doping profile structures whose realization requires the implementation of one or two highly doped spikes limiting the avalanche zone width. Those

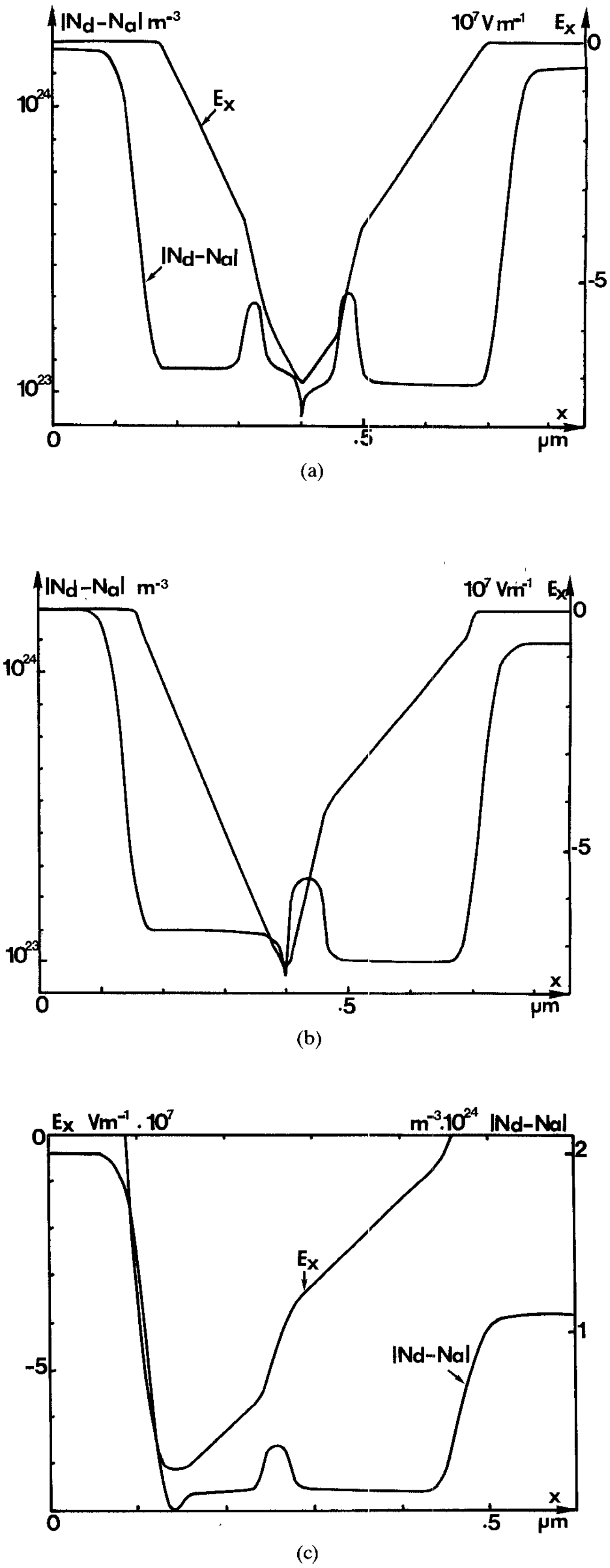

Fig. 1. Doping profile $|N_d - N_a|$ and associated static electric field internal distribution of the various kinds of 94 GHz Read structures. (a) Optimum double Read structure DR1 ($T = 500$ K, $V_0 = 17.5$ V, $J_0 = 6$ kA/cm^2). (b) Optimum hybrid double Read structure HDR1 ($T = 500$ K, $V_0 = 18.7$ V, $J_0 = 21$ kA/cm^2). (c) Optimum single-drift Read structure SDR1 ($T = 500$ K, $V_0 = 14.3$ V, $J_0 = 0.02$ kA/cm^2). (*Continued on next page.*)

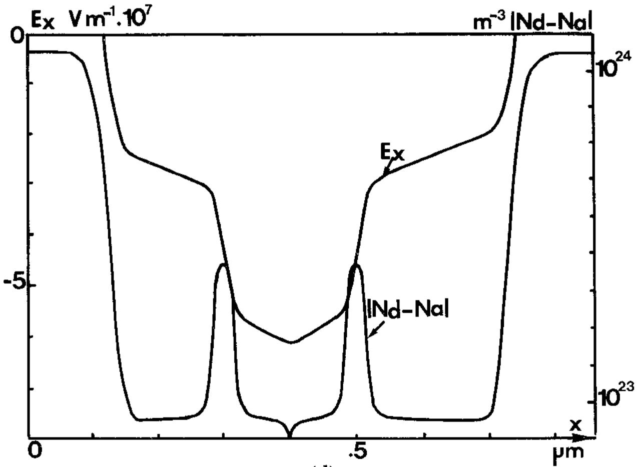

(d)

Fig. 1. (*Continued*) (d) Typical low doped transit zone double Read structure DR2 ($T = 500$ K, $V_0 = 22$ V, $J_0 = 19.5$ kA/cm^2).

exhibiting a spike in both the p and n zones will be named double Read structures (DR) while those exhibiting a spike in the n zone and a uniform doping profile in the p zone will be called hybrid double Read structures (HDR). In addition, in order to complete the study, both flat doping and Read doping profile single-drift structures have been considered (referred to respectively as SDR2 and SDR1). Moreover, in order to clarify the discussion, two typical but nonoptimized double-drift structures have been added (called DDR2 and DR2).

Note that the structure optimization method is not detailed in this paper but is similar to those previously presented for the double-drift flat doping profile [6]. In the case of Read doping profile structures, the minimum avalanche zone width has been limited to 0.2 μm in order to limit the magnitude of the electric field in this zone and consequently to minimize the unfavorable carrier injection by tunneling. Indeed this additional conduction current is in phase with the local RF voltage [12]. Moreover this allows us to minimize the premature collapse of the avalanche process due to space charge effects. The technological parameters of the structures considered are summarized in Table I and Fig. 1, which show both their respective doping level and static electric field spatial distribution.

IV. Optimization Conditions of the Structures

The RF performance of the different structures must be compared according to realistic and identical operating parameters. Under high power operation the diode junction temperature rise constitutes the fundamental limitation of IMPATT operation. Indeed the device reliability is strongly dependent on this parameter. Consequently the maximum junction temperature has been fixed at 227°C (500 K) according to an ambient temperature of 20°C. Thus the diode reliability can be guaranteed for a wide range of external temperatures.

Secondly all the structures have been optimized according to a terminal negative resistance level of -1.5 Ω. This value is high enough to minimize the influence of parasitic RF losses on the oscillator RF output performance and to overcome the problems of diode impedance matching to the loading circuit. Thus, the optimum diode area has been found to be close to 10^{-9} m^2 for each kind of structure. Consequently this value has been retained for the comparison. So the corresponding optimum thermal resistance value is of the order of 35°C/W for a diode thermocompressed on a diamond II A heat sink and close to 70°C/W for a diode mounted on a gold heat sink [9]. In addition, it can be seen that a lossy resistance on the order of 0.12 Ω, corresponding to the resistance of the highly doped regions of the collectors, is already naturally taken into account in the simulations.

V. Main Results

Fig. 2 illustrates the RF performance of the various structures as a function of the terminal negative resistance level (and consequently implicitly as a function of the RF voltage modulation rate). Recall that in these simulations the dc bias current density has been adjusted with respect to the imposed junction operating temperature.

The first point to be noted is that optimized single-drift structures (SDR1 and SDR2) exhibit an interesting power level close to 1 W associated with a 15% conversion efficiency. However, double-drift structures confirm their superiority, especially when the loading resistance value increases.

Concerning the flat doping profile double-drift structures, the optimization of their technological characteristics (both the doping level and the dimensions of the p and n zones) has pointed out the superiority of a highly doped punch-through structure (DDR1) compared to a structure in which the transit conditions of the electron and hole bunches have been optimized at 94 GHz without accounting for thermal limitation (DDR2). Indeed, a high doping level minimizes the operating dc bias voltage so that higher dc bias current densities can be achieved for an identical junction temperature rise.

In the case of the double Read structures, the influence of the transit zone doping level on the RF performance of the diode has been extensively investigated. As for the flat doping profile structures the paramount importance of the dc bias current density was confirmed since highly doped transit zone structures (DR1) were found to be more powerful than lower doped transit zone classical ones in which the electron and hole bunches are moving at saturated velocity in a nearly uniform electric field (DR2) [13]. Indeed, the RF performance of these structures has been found to be limited by the unfavorable influence of three related effects:

- The voltage across the electron and hole transit zones and consequently the diode total dc bias voltage vary as the inverse of the doping level in these zones. This effect is not negligible when the thermal limitation is strictly taken into account.

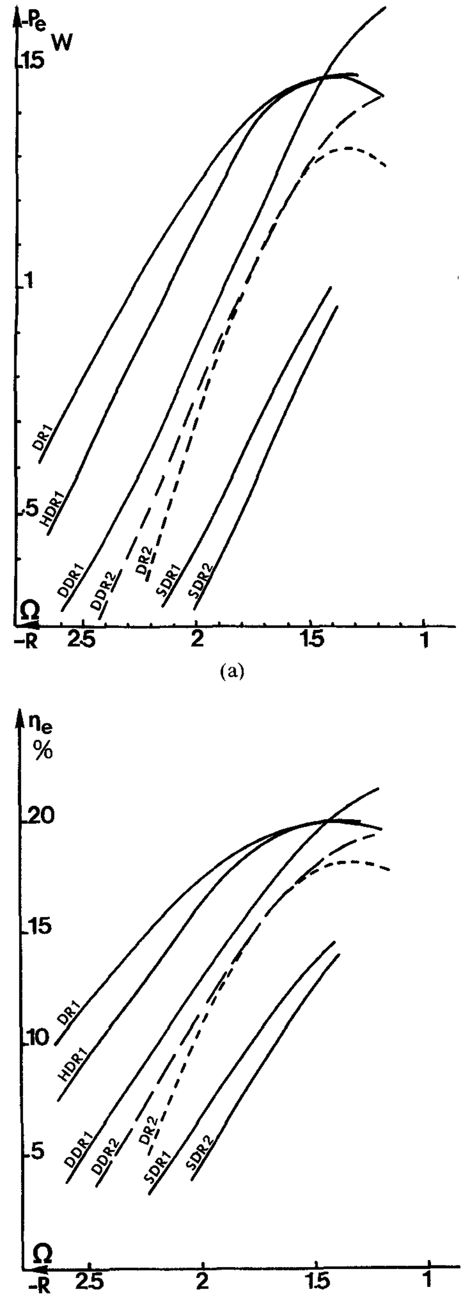

Fig. 2. (a) RF power level P_e and (b) associated efficiency η_e for the various 94 GHz single- and double-drift structures as a function of the terminal negative resistance level R in the case of diamond II A heat sink. The bias current is adjusted to fulfill the constant temperature requirement. $R_{th}=35°C/W$; $T_j=500$ K; $T_a=20°C$; $S=10^{-9}$ m^2; $f=94$ GHz.

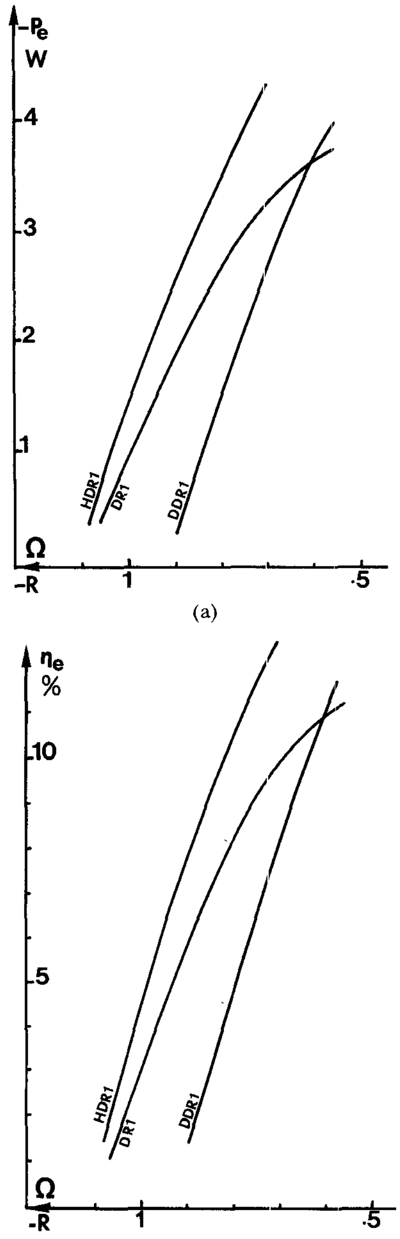

Fig. 3. (a) RF power P_e and (b) associated efficiency η_e of the 94 GHz optimum double-drift structures as a function of the terminal negative resistance level R in the case of gold heat sink. Conditions are the same as in Fig. 2. $R_{th}=70°C/W$; $T_j=500$ K; $T_a=20°C$; $S=10^{-9}$ m^2; $f=94$ GHz.

- The space charge reaction effects in the transit zones induced by the high dc bias current densities required at millimeter-wave frequencies are more pronounced when the transit zone doping level is low.
- The maximum RF power is reached for high RF voltage modulation drive. However the low doped transit zone double Read structures are more sensitive to the modulation of their depleted zone under RF voltage swings. Indeed, when the instantaneous RF voltage reaches its minimum value the electric field intensity becomes very low in the transit zones and can even be reversed in sign, thereby yielding a dispersion of the electron and hole bunches and a collapse of the RF power generation. This effect has been previously described [14], [3].

The comparison between the theoretical performances of the various kinds of double-drift structures appears more complicated since it depends on the RF power level range. From a general point of view the results show that the Read doping profile structures exhibit higher RF performance than the flat doping profile ones at high terminal negative resistance levels and thus at moderate output power levels. But when looking for maximum output power levels the interest of double Read structures tends to vanish. It can be noticed that the hybrid double Read structure includes advantages of both the double Read and flat doping profile structures. Indeed it presents higher performance than flat doping profile ones at a high terminal negative resistance level and reaches a maximum RF performance level similar to that of the double Read structure.

Concerning the maximum achievable RF power level, the flat doping profile double-drift structure appears as potentially the most powerful structure since it can provide an RF power level of about 1.6 W with a conversion efficiency close to 21.5%; these values are of the order of 10% higher than those of the maximum Read doping profile structures.

The main interest of the Read doping profile structures derives from the fact that they retain a high terminal negative resistance level for low and medium RF power levels. Consequently they appear well suited for the realization of reliable medium-power gold heat sink diodes. Indeed since in this case the thermal resistance is at least twice as high as for the case of diamond heat sinks, the thermal limitation is more stringent and the device must operate at a lower dc bias current density and at lower RF voltage modulation ratios in order to keep the terminal resistance at an acceptable level. Fig. 3 shows the RF performance of the optimum double-drift structures when a 70°C/W thermal resistance is considered. Note in this case the low terminal negative resistance levels. Consequently the RF performance will be drastically dependent on the RF losses and diode impedance matching. The superiority of Read doping profile structures over flat doping ones is confirmed but the hybrid double Read one surprisingly appears as the most powerful. However one must bear in mind that the structures were optimized for low thermal resistance and thus for high dc bias current density.

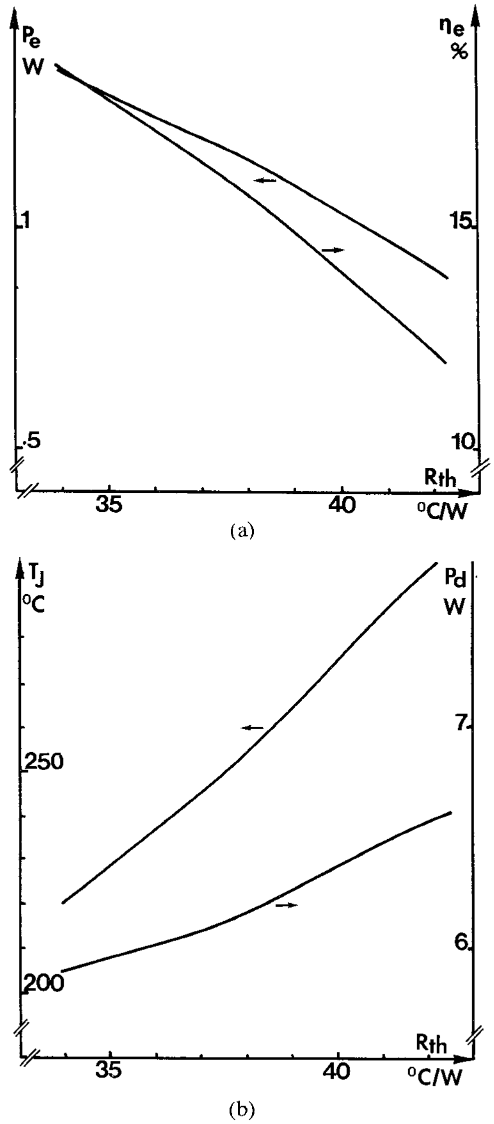

Fig. 4. (a) RF power P_e and associated efficiency η_e for the DDR2 structure as a function of the thermal resistance R_{th} when the dc bias current density is kept constant. $S = 10^{-9}$ m^2; $R = -1.5$ Ω; $J_0 = 31.2$ kA/cm^2; $T_a = 20$°C. (b) Corresponding junction operating temperature T_j and Joule dissipated power P_d when the dc bias current density is kept constant.

VI. Influence of the Thermal Resistance and RF Losses

The theoretical results presented above have pointed out extremely high RF power levels associated with high conversion efficiencies. These results appear to be surprisingly higher than the present experimental ones. However they have been obtained with optimum thermal resistances and without RF losses. As the IMPATT oscillators are mainly thermally limited we have quantified the influence of the diode thermal resistance on its RF performance.

For this purpose Fig. 4 presents as an example the RF power level and conversion efficiency of the flat doping profile diode DDR2 as a function of the thermal resistance value. In this case the dc bias current density was kept constant. The results show that the RF performance decreases when the thermal resistance increases since the junction operating temperature increases. An increase of 5°C/W in the thermal resistance over the optimum value of 35°C/W yields a degradation of about 20% of the power and 25% for the diode conversion efficiency. The corresponding junction temperature increase is about 50°C. If now, in order to ensure safe operation, the junction operating temperature is kept constant the degradation of the RF performance is more drastic when the thermal resistance increases. Indeed, in order to maintain a constant junction temperature the dc bias current has to be decreased when the thermal resistance increases and we have seen previously the paramount importance of this operating parameter: the higher the current density the higher the output power. This is illustrated in Fig. 5. For the same thermal resistance increase of 5°C/W the output power decrease reaches 30%.

Since the output power increases with the RF voltage swing, the highest RF power levels are obtained at low diode terminal negative resistance levels. Consequently the

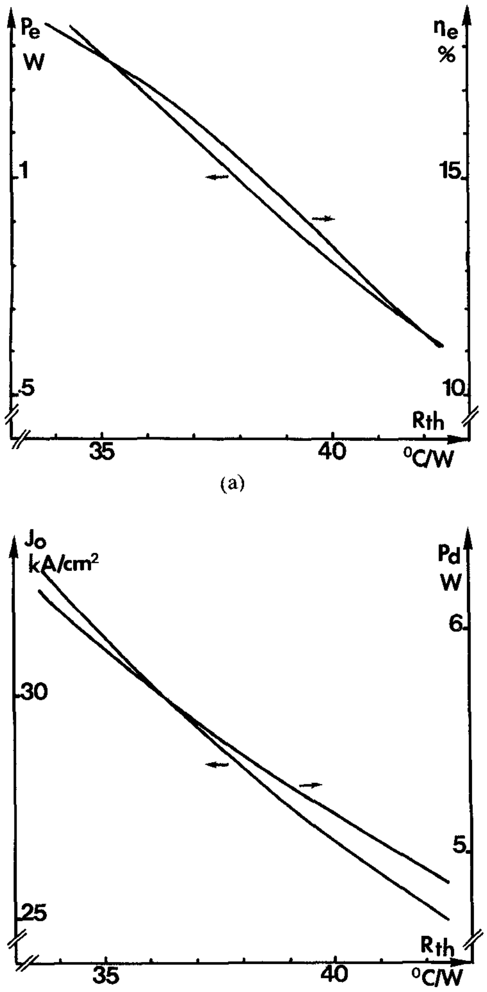

Fig. 5. (a) RF power level P_e and associated efficiency η_e for the DDR2 structure as a function of the thermal resistance R_{th} when the junction temperature is kept constant. $S = 10^{-9}$ m^2; $R = -1.5$ Ω; $T = 500$ K; $T_a = 20$°C. (b) Corresponding decrease of the dc bias current J_0 and Joule dissipated power P_d with increasing thermal resistance for a constant junction temperature.

influence of the RF losses must be taken into account. These latter result mainly from the diode package and the RF loading circuit. They can be simply taken into account by means of an additional lossy resistance. This parasitic series resistance has a drastic influence on the diode performance. When a high-efficiency cavity is used (waveguide circuits) the flat doping profile structures still behave well and remain as powerful as double Read structures [13]. If more lossy circuits are used, such as planar ones, then the higher negative resistance level of double Read diodes makes them the best candidate for high-power millimeter-wave operation.

VII. Conclusion

The potential RF performances of the various types of silicon IMPATT homojunction structures (single and double drift, flat and Read doping profile structures) have been systematically investigated in order to define the one that is most efficient for the realization of reliable, high-power, high-efficiency CW power sources in the 94 GHz propagation window. This comparison has been carried out by means of an accurate numerical IMPATT oscillator model accounting in a self-consistent manner for both the thermal limitation and the diode impedance matching conditions.

The optimization of the technological parameters of each structure has been performed, with particular attention paid to reliability (limited junction temperature) and the RF losses (high diode terminal negative resistance level). This study has yielded the optimum RF performance of the different Read and flat doping profile structures considered according to optimum operating conditions since minimum values of both the thermal and series resistances have been taken into account. Concerning the maximum achievable RF power levels, the results show that, in contrast to lower operating frequencies, Read doping profile structures do not improve the RF performance level in comparison to the flat doping profile ones. However, because of their intrinsic RF properties, Read doping profile structures, especially the hybrid double Read ones, appear to be the most efficient structures in the case of higher thermal resistance medium-power gold heat sink diodes. Under optimum operating conditions extremely high emitted RF performance has been predicted. A maximum theoretical power level of the order of 1.6 W associated with a conversion efficiency of 21.5% and a −1.2 Ω diode terminal negative resistance has been computed for the optimum double-drift flat doping profile structure.

The influence of the two main limiting parameters, the diode thermal resistance and RF circuit losses, has been investigated. These results allow us to explain the discrepancy observed between the theoretical predictions and the present experimental findings. A drastic degradation of the RF performance with increasing thermal resistance has been pointed out, especially when a safe junction operating temperature is required. The influence of the RF losses has been quantified. The results show that all the double-drift structures exhibit similar RF performance, but the flat doping profile structures present a slight superiority in the case of low-loss RF circuits while the Read doping profiles benefit from their higher terminal resistance level in the case of more lossy RF circuits. However for a final choice certain technological considerations must be taken into account and the relative simplicity of flat doping profile structures could be an important factor.

Finally, on the basis of theoretical results and future expected technological improvements, the realization of W-band silicon IMPATT oscillators able to provide a CW output power greater than 1 W with conversion efficiencies higher than 10% at safe junction temperature rise can be realistically expected if thermal resistance reaches its minimum theoretical value.

References

[1] T. Midford and R. Bernick, "Millimeter-wave CW IMPATT diodes and oscillators," *IEEE Trans. Microwave Theory Tech.*, vol. MTT-27, pp. 483–492, May 1979.

[2] R. K. Mains and G. I. Haddad, "Properties and capabilities of millimeter-wave IMPATT diodes," *Infrared and Millimeter Waves*, vol. 10, pp. 110–231, 1983.

[3] C. Dalle, D. Degrugillier, J. L. Nieruchalski, D. Lippens, and P. A. Rolland, "Capabilities of IMPATT diodes in the millimeter-wave frequency range," in *Proc. IEEE/Cornell Conf. Advanced Concepts in High Speed Semiconductor Devices and Circuits*, (Ithaca), July 1985, pp. 351–359.

[4] R. S. Ying, "Solid-state sources power millimeter transmitters," *Microwave Syst. News*, vol. 13, no. 12, pp. 280–286, Nov. 1983.

[5] M. Heitzmann and M. Boudot, "New progress in the development of a 94 GHz pretuned module silicon IMPATT diode," *IEEE Trans. Electron Devices*, vol. ED-30, pp. 759–763, July 1983.

[6] C. Dalle, G. Lleti, and P. A. Rolland, "Flat doping profile double drift silicon IMPATT for reliable CW high power high efficiency generation in the 94 GHz window," *IEEE Trans. Electron Devices*, to be published.

[7] B. Culshaw, R. A. Giblin, and P. A. Blakey, "Avalanche diode oscillator II. Capabilities and limitations," *Int. J. Electron.*, vol. 39, no. 2, pp. 121–172, 1975.

[8] J. F. Luy, E. Kasper, and W. Behr, "Semiconductor structures for 100 GHz silicon IMPATT diodes," in *Proc. 17th European Microwave Conf.* (Rome), Sept. 1987, pp. 820–825.

[9] J. F. Luy, E. Kasper, and W. Behr, "Silicon MBE made IMPATT diodes," presented at Workshop MTT Chapter of West Germany Section of the IEEE, Ulm, Sept. 1987.

[10] B. Culshaw, R. A. Giblin, and P. A. Blakey, "Avalanche diode oscillator I. Basic concept," *Int. J. Electron.*, vol. 37, no. 5, pp. 577–632, 1974.

[11] C. Dalle and P. A. Rolland, "Drift-diffusion versus energy model for millimeter wave IMPATT diodes modelling," *Int. J. Numer. Modelling, Electronic Networks, Devices and Fields*, to be published.

[12] E. O. Kane, "Theory of Tunneling," *J. Appl. Phys.*, vol. 32, pp. 83–91, 1961.

[13] M. El-Gabaly, R. Mains, and G. Haddad, "Effect of doping profile variation on GaAs hybrid and double-Read IMPATT diode performance at 60 and 94 GHz," *IEEE Trans. Microwave Theory Tech.*, vol. MTT-32, pp. 1342–1352, Oct. 1984.

[14] R. Mains, G. Haddad, and P. Blakey, "Simulation of GaAs IMPATT diodes including energy and velocity transport equations," *IEEE Trans. Electron Devices*, vol. ED-30, pp. 1327–1338, Oct. 1983.

[15] A. Derycke and G. Salmer, "Circuit analysis and design of radial pretuned modules used for millimeter-wave oscillators," *IEEE Trans. Microwave Theory Tech.*, vol. MTT-33, pp. 600–609, July 1985.

Christophe Dalle was born in Cambrai, France, on January 11, 1958. He joined the Centre Hyperfréquences et Semiconducteurs of Lille in 1982. He received the doctorat en électronique from the University of Lille Flandres Artois in July 1986 on the modeling of p–n junction devices and avalanche diodes for direct and harmonic RF generation in the millimeter-wave range.

Since October 1986 he has been with the Centre National de la Recherche Scientifique, where he is working in the field of millimeter-wave active devices and subsystems.

Paul-Alain Rolland was born in Bangui, Central African Republic, on June 24, 1947. He received the degree of Electronical Engineer in 1970 and the These d'Etat degree in 1978.

He is currently Professor at the Technical University of Lille, where he is responsible for the microwave section of the University Engineer School (EUDIL) and manager of the millimeter-wave research team at the Centre Hyperfréquences et Semiconducteurs (CHS). He is mainly involved in the modeling and realization of millimeter-wave devices and subsystems.